

Thermal evolution of a silicone resin/polyurethane blend from preceramic to ceramic foam

T. TAKAHASHI, H. MÜNSTEDT*

Lehrstuhl für Polymerwerkstoffe, Universität Erlangen-Nürnberg, Martensstraße 7, D-91058 Erlangen, Germany
E-mail: polymer@ww.uni-erlangen.de

P. COLOMBO

Dip. di Chimica Applicata e Scienza dei Materiali, Università di Bologna, Viale Risorgimento, 2, I-40136 Bologna, Italy

M. MODESTI

Dip. di Processi Chimici dell'Ingegneria, Università di Padova, via Marzolo 9, I-35131 Padova, Italy

Ceramic foams, prepared by the pyrolysis of a foamed blend of a methylsilicone preceramic polymer and a polyurethane, exhibit excellent mechanical properties. The thermal evolution of process to produce from the foamed blend (weight ratio of 1 to 1) to ceramic foam was investigated from room temperature to 1400°C. Firstly, the methylsilicone preceramic polymer was characterized with various techniques. Secondly, the weight decrease and the degradation gas from the unpyrolyzed foamed blend, the phase morphology change, the compositional change, and the dimensional change were investigated. The main variation of characteristics of the foamed blend was observed in the temperature range 400 to 600°C, where the largest weight loss occurred in TGA, for most of the measurements. At these temperatures, the decomposition of the polyurethane phase is mostly completed, and the polymer-to-ceramic conversion of the silicone resin is under way. The phase-morphological analysis surprisingly showed that the polyurethane was dispersed as particles in a methylsilicone preceramic polymer matrix, although originally polyurethane was intended to be used as a sacrificial template matrix. The polyurethane domain particles gradually aggregated and tended to disappear as the temperature increased, and the ceramic foam walls and struts appeared to be dense (for pyrolysis temperature <1400°C). These features can be explained assuming that the preceramic polymer matrix deformed during the decomposition of the polyurethane and the polymer-to-ceramic conversion. © 2001 Kluwer Academic Publishers

1. Introduction

The processing of ceramic materials in the system Si-O-C from organosilicon preceramic polymers has received considerable attention [1–4], since a breakthrough was made by Yajima *et al.* in the invention of SiC based fiber from polycarbosilane in the 1970s [5]. The main advantages of the preceramic polymer route over the conventional ceramic process come from two points, namely the lower processing temperature (usually <1500°C) and wider possibilities of product shaping, such as, fibers, films, membranes, bulk components, and foams.

Because of easy handling characteristics in ambient atmosphere, polysiloxanes have been frequently studied since White *et al.* reported in 1987 [6, 7]. Polysilox-

ane ceramic precursors have been usually referred to as silicone resins [8, 9], which is a nonlinear three-dimensionally cross-linked polymer containing largely silsequioxane, whose formula is $\text{RSiO}_{3/2}$, where R is typically an hydroxyl, alkoxy, alkyl or phenyl group. The conversion from silicone resin to ceramic occurs with large shrinkage and weight decrease, which typically limit the applications only to small-dimensional products (fibers and coatings). With the development of key related technology in recent years, it has nevertheless become possible to expand the versatility of the process using silicone resins [10–15].

New processing technologies in which organic polymers, as processing aids or sacrificial template matrices, have been mixed with inorganic ceramic components,

* Author to whom all correspondence should be addressed.

either ceramic powder or an inorganic monomer, have been proposed in recent years [16–23]. The concept has already been utilized for production in injection molding machines or for making uniquely shaped products [10–12, 16–23]. The key point is that the organic polymer helps the shaping process and then disappears during heating; the amount of organic component used depends of course on the role it has in the process (e.g. binder, volatile matrix, etc.).

Bulk components can be fabricated: for instance alumina parts are obtained from the blend of organic polymers (e.g., polybutylmethacrylate, polyethylene-vinylacetate, etc.) and alumina powder through melt compounding, shaping by injection molding, and sintering around 1600°C [16]. Tape casting of a slip made from the mixture of alumina powder, methylmethacrylate (MMA) and initiator through *in situ* polymerization and sintering at 1600°C, the so called gel-casting process [17] should also be mentioned. Porous ceramics have also been fabricated, for instance using the gel-casting process [18] or the polymer-sponge method, where an organo-polymeric sponge is dipped into a ceramic slurry and then the organic component is removed by sintering [19]. Using the sol-gel method [24, 25] and hybrid organic/inorganic structures, ceramics with various degrees of porosity have been obtained by removing the organic component [20–23].

Recently, Colombo and Modesti developed a novel processing method for producing ceramic foams [10–12], through the pyrolysis under an inert gas of foamed polymer blends of a preceramic polymer, i.e. a silicone resin, and an organic polymer, i.e. polyurethane (PU). The main concept behind this technology is the combination of polyurethane, which is known to be easily foamed (physical or chemical blowing) and can act as a structural template, and silicone resins, which can be mixed in solution with the polyurethane precursors [10–12].

The bulk density of the foams ranges from 0.2 to 0.6 g/cc; cell size varies between 100 and 700 micron [10–12]. Flex strength, crushing strength, and elastic modulus increase with higher density, and values up to 14 MPa, 16 MPa, and 8 GPa, respectively, have been obtained [10–12]. The foams possess a coefficient of thermal expansion of $0.2 \times 10^{-6} \text{ K}^{-1}$ (20–1000°C) and display excellent thermal shock resistance properties [10–12].

Understanding the decomposition process as well as the role of PU in developing a desired morphology is very important, if one wants to produce ceramic foams for different applications (e.g. filters, thermal shields, catalytic substrates, lightweight structural components), all requiring a specific, tailored structure (open or closed cell, various porosity sizes and ranges, etc.). In this paper, the thermal evolution from the foamed blend of methylsilicone preceramic polymer and polyurethane to ceramic foam, as well as the phase morphology at room temperature, have been studied with different analytical techniques (TGA-FTIR (thermal gravimetric analysis—Fourier transform infrared spectroscopy), SEM (scan-

ning electron microscopy), FTIR spectroscopy and dilatometry).

2. Experimental

2.1. Materials

Polyurethane (PU) foam was prepared from polyether polyol, amine catalyst, solvent, surfactant and polymeric isocyanate. The polyol mixture was comprised of two polyether polyols (Tercacol 3 (hydroxyl number: 56 mg of KOH/g, viscosity at 25°C : 500 mPa · s, $M_w = 3000$ g/mole) and Tercarol 1 (hydroxyl number: 168 mg of KOH/g, viscosity at 25°C : 280 mPa · s, $M_w = 1000$ g/mole), supplied by Enichem). The amine catalysts were bis(dimethylaminomethyl)ether and triethylenediamine in dipropylene glycol (Niax A-1 and A-33, supplied by OSi Specialties). The solvent was dichloromethane. The surfactant was polydimethylsiloxane (SC250 and SH205, supplied by OSi Specialties). The isocyanate was polyphenylmethane isocyanate (Tedimon 31, viscosity at 25°C : 180 to 250 mPa · s, %NCO : 31, supplied by Enichem). The reaction between the polyol mixture and the isocyanate gives rise to a semirigid PU, as reported in previous papers [10–12].

The preceramic polymer used here was a methylsilicone resin (SR350, General Electric Silicone Products Division, Waterford, NY). It is known that the methylsilicone resin can be converted to silicon oxycarbide (SiOC), that is an amorphous ceramic material in which Si atoms are bonded to both O and C atoms, by pyrolysis between 1000 and 1500°C under inert atmosphere [26–29].

The foamed PU was prepared by the generation of CO₂ gas by addition of water into the mixture of the polyols, the amine catalysts, the surfactant, the isocyanate and the solvent (chemical blowing). The foamed blend of SR350 and PU, with a weight ratio of 1 to 1, was prepared in two steps. The first step was the addition of SR350 dissolved in CH₂Cl₂ to the mixture of the polyols, the amine catalysts, the surfactant, and additional dichloromethane. The second step was the addition of polyisocyanate to the solution obtained in the first step. The expansion started during mechanical stirring by the evaporation of the solvent caused by the exothermal reactions occurring in the solution (physical blowing). In addition to that, water generated by the condensation reaction, promoted by the amine catalyst, of Si-OH groups in the silicone resin reacted with isocyanate, giving carbon dioxide gas that participated in the foaming (chemical blowing) [10]. Not only urethane bonds but also ureic bonds are formed through the reaction. It has to be mentioned that the silicone resin was pre-treated at 150°C before dissolving into dichloromethane, in order to reduce the amount of Si-OH groups present. The detailed preparation procedure has been already reported in previous papers [10–12].

The foamed blend of SR350 and PU was pyrolyzed under nitrogen (99.999% N₂, 5.0 cc/min) at the heating rate of 2 K/min up to various temperatures. The same samples were kept for 1 h at final pyrolysis temperatures of 200, 300, 400, 600, 800, 1000, 1200, and

1400°C. These samples were used for SEM and FTIR spectroscopy analysis, mentioned later.

2.2. Characterization of as-received SR350 silicone resin

It has been reported in the literature [26] that the starting materials for the synthesis of SR350 are 2 to 8% of dimethyl dichlorosilane and 92 to 98% of methyl trichlorosilane. The main features of SR350 before and after pyrolysis were characterized by Renlund *et al.* [26]. To our best knowledge, however, there have been few fundamental studies of the silicone resin before cross-linking. The features of SR350 (as received) were, therefore, characterized by GPC, DSC, XRD, and by rheological measurements. For the characterization of molecular weight and molecular weight distribution, GPC (gel permeation chromatography) was used at room temperature.

The thermal properties of SR350 were characterized with DSC (differential scanning calorimetry, DSC 2920, TA Instruments). The DSC analysis was carried out under conditions at which no cross-linking reactions occur (below 100°C). The dynamic mechanical behavior in shear [30, 31] was measured for SR350 melt using a strain-controlled rheometer (ARES, Rheometrics Scientific). The used configuration was parallel plates with 25 mm of diameter. The microstructure of SR350 before pyrolysis was analyzed using XRD (X-ray diffraction, CuK α radiation, Diffractometer-5000, Siemens) at room temperature.

2.3. Analysis of the decomposition products

TGA-FTIR (thermal gravimetric analysis connected with Fourier transform infrared spectroscopy) was used for the analysis of weight loss and decomposition gases of SR350, foamed PU, and foamed blend of SR350/PU. The TGA measurements (thermal gravimetric analysis, TGA2950, TA Instruments) were conducted from room temperature to 1000°C, while the decomposition gases coming from the TGA cell were qualitatively analyzed with a FTIR spectrometer (Magna-IR Spectrometer 750 with TGA interface, Nicolet). TGA analysis was performed using 70 ml/min of nitrogen (99.999% purity) flow and a heating rate of 10 K/min. The decomposition gases were transferred to the gas cell in the FTIR instrument through a transfer tube. The FTIR spectra were collected with a resolution of 4 cm⁻¹ for 32 scans. Foamed PU and foamed SR350/PU were dried at 60°C under vacuum for 3 hours to eliminate CH₂Cl₂ completely before performing the measurement.

2.4. Phase morphology analysis

The phase morphology of foamed blends of SR350/PU before and after pyrolysis at various temperatures (200, 300, 400, 600, 800, 1000, 1200, 1400°C) was characterized by SEM (Stereoscan 250 MK3, Cambridge Instruments). Elemental analysis (EDX) was also conducted to clarify which of the observed phases contained the pyrolysis residues of the SR350 silicone resin.

2.5. Compositional and dimensional changes

The thermal evolution of the foamed blend of SR350/PU as a function of temperature was characterized following the compositional and dimensional changes and the variation in bulk (apparent) density and in the average cell dimension. The compositional change of the bulk was analyzed by FTIR spectroscopy. The linear dimensional variation of the foamed blend was measured using a Netzsch 402E dilatometer in flowing nitrogen at the heating rate of 10 K/min. The bulk density of the foams was computed from the weight-to-volume ratio, while the true density was measured using a pycnometer. The thermal evolution of cell size as a function of temperature was characterized using SEM, and the cell dimensional analysis was carried out using an image analysis software (Kontron Vidas image analyzer).

3. Results and discussion

3.1. Main characteristics of SR350 before cross-linking

SR350 starts cross-linking as the temperature increases above a certain level [26]. The temperature range in which SR350 does not show a cross-linking reaction was carefully determined by a rheological method, since the viscosity increases sharply when cross-linking occurs. No reaction was found below 100°C within 15 minutes, where the first and the second heating of DSC was measured for SR350 (Fig. 1a). For the first heating an onset transition temperature at 54.1°C and a small peak at 55.8°C were found. For the second heating, only the onset transition temperature at 42.6°C was observed. No melting peaks were present in the temperature range between -50 and 100°C. This curve shape is typical of amorphous polymers, and SR350 can be considered as an amorphous polymer from the point of view of DSC. Since it is known that the small peak observed during the first heating reflects the preheating history, the glass transition temperature was estimated, from the second heating, to be 42.6°C. The glass transition temperature of SR350 was similar to those of other commercially available silicone resins, which were all between 37 and 46°C [32].

From the GPC analysis of SR350, the number and weight averaged molecular weight (M_n , M_w) were found to be 1.5×10^3 and 6.6×10^3 g/mole, respectively. The polydispersity index (M_w divided by M_n) is 4.4. This means that the average molecular weight of SR350 is relatively low and SR350 contains substantial amounts of species with molecular weights lower than 1000 g/mole, which can easily be evaporated. Molecular weight analysis of various commercially available silicone resins (methyl- and methylphenyl- silicone resins, product names: MK and H44 from Wacker Chemie, Germany) showed that M_w was 9.4×10^3 and 2.1×10^3 g/mole, and M_w/M_n was 3.6 and 1.8, respectively [32]. One can thus say that the molecular parameters of SR350 resemble those of other commercially available silicone resins [32].

As it can be seen from Fig. 1b, XRD of SR350 before cross-linking shows two peaks located at 10.5 and

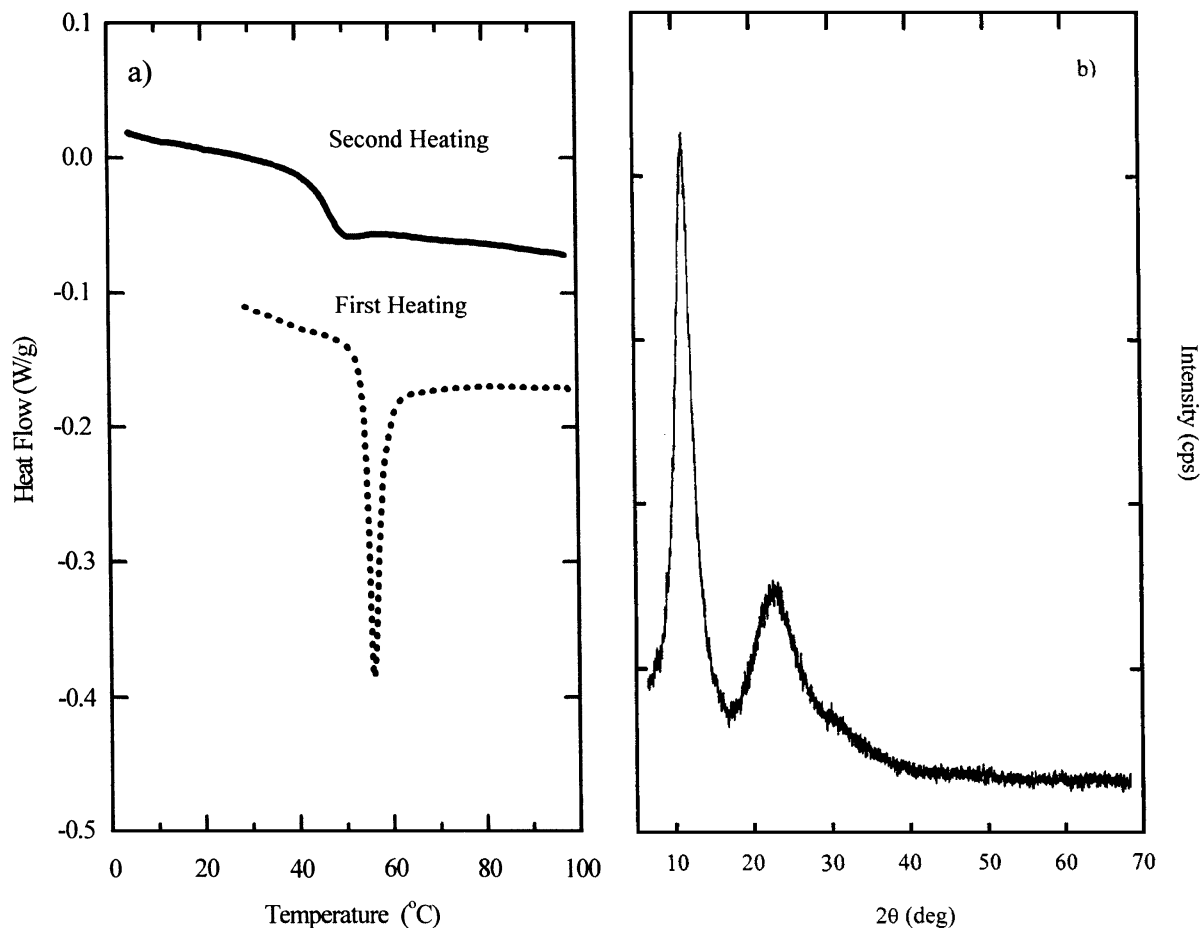


Figure 1 (a) DSC curves of SR350 (as received) for the first (dotted curve) and the second heating (solid curve). The second heating curve is transferred by +0.1 W/g. (b) XRD pattern for SR350 (as received).

22.4 deg. The broad peak at 22.4 deg in Fig. 1b can be attributed to the amorphous SiO_2 structure [33]. The peak at 10.4 deg suggests the existence of a relatively regular structure with lattice spacing of 8.5 Å. The presence of two similar peaks was also found in the XRD patterns of several commercially available silicone resins, and the lattice spacing calculated from the first peak increased with the size of organic groups [32]. In addition, two peaks were also present in the molten stage [32]. The most likely explanation for the existence of these two peaks is that the silicone resins contain not only an amorphous random structure, but also a relatively regular structure, such as a broken ladder [34] or a partial cage [6, 32]. These hypothetical structures are presented in a literature [8].

Viscoelastic properties of linear not-entangled polymers, that have molecular weight less than M_c ($M_c = 2M_e$, M_e : entanglement molecular weight [35]), have been extensively studied [30, 36]. In the double-logarithm plot of storage modulus G' and loss modulus G'' as a function of frequency, it is known that the G'' is proportional to the frequency, and that the slope of G' is 2 in the low frequency terminal zone [30, 36]. The M_e of linear polydimethylsiloxane was reported to be 8160 g/mole at 20°C [35]. Taking this fact into consideration, one can conclude that SR350 contains almost no entanglements. If the former experimental evidence [30, 36] about the not-entangled linear polymers can be extrapolated to SR350, slopes

of 2 and 1 for G' and G'' in the low frequency terminal zone should be easily expected.

The rheological measurements were conducted under the conditions, below 100°C and within 15 minutes, where no cross-linking reaction occurs. The critical strain for leaving the linear region of the experiments was carefully checked. All dynamic mechanical experiments were carried out in the linear range. The measuring temperatures were 70, 80, 90, and 100°C. Fig. 2a displays the master curves of G' and G'' for SR350 at the reference temperature of 90°C. A time-temperature superposition based on the WLF (Williams-Landel-Ferry) rule [30] was successfully applicable. G'' is proportional to the frequency in the terminal region, however, the slope of G' is 1.5 and 1.0 in the high and low frequency regions, respectively. The G' curve exhibits a bending in an intermediate region. These characteristics were also found for other commercially available silicone resins [32]. The feature of the G' curve was quite unexpected, starting from the idea that the silicone resin was a not-entangled polymer. The slope of the curve reminds one of gel polymer systems [37] or of filled polymers [38]. The rheological measurements thus suggest that SR350 is a heterogeneous mixture, where rigid regular nano-structures (detected by XRD, see peak at 10.4°) may build up a physical cross-linking network in the amorphous random structure. From DSC, GPC, XRD and rheological results, it can be interpreted that SR350 is an amorphous low molecular

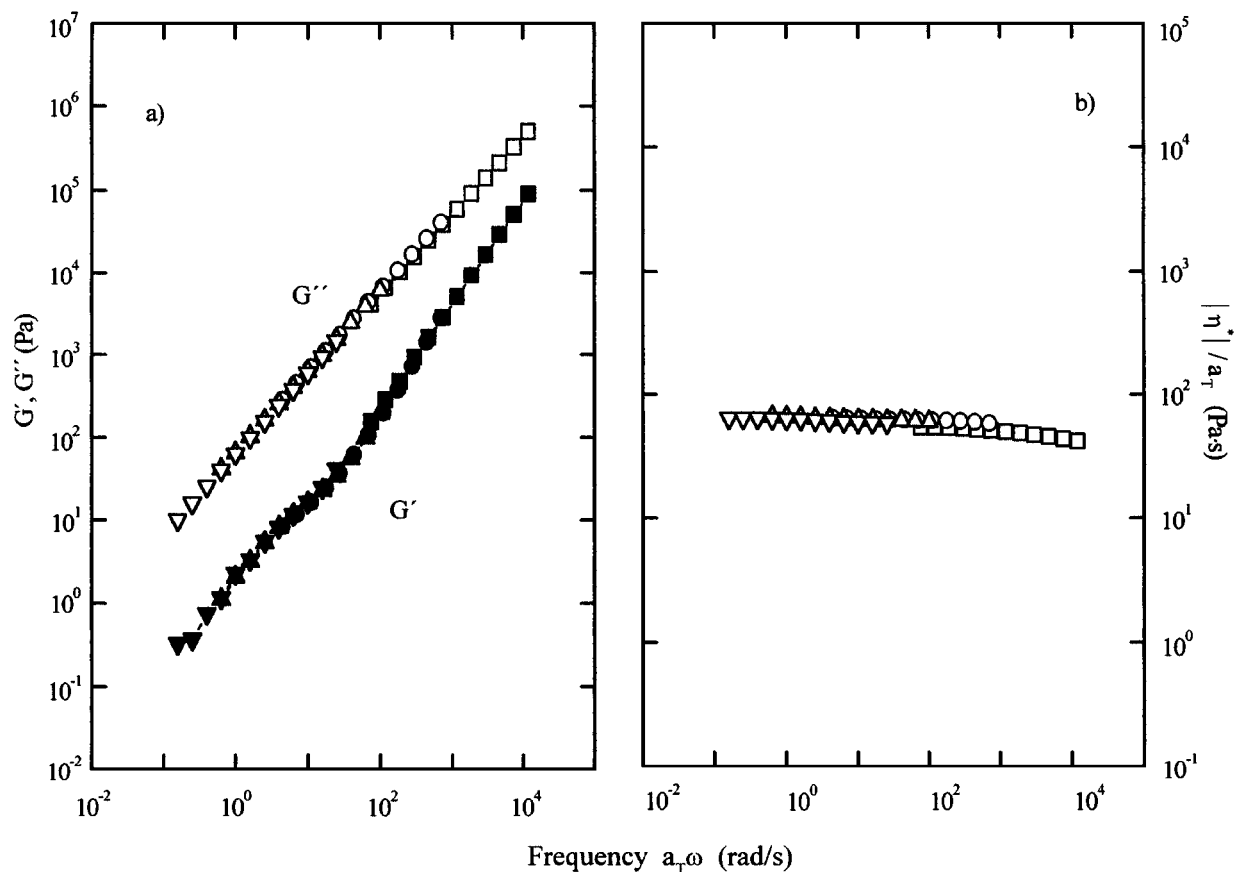


Figure 2 (a) Master curves of storage modulus G' (closed symbols) and loss modulus G'' (open symbols) for SR350 (as received) measured at various temperatures: (■, □) 70°C, (●, ○) 80°C, (▲, △) 90°C, (▼, ▽) 100°C. The reference temperature is 90°C. (b) Master curve of complex viscosity $|\eta^*|$ for SR350 (as received) measured at various temperatures: (□) 70°C, (○) 80°C, (△) 90°C, (▽) 100°C. The reference temperature is 90°C.

polymer, that has a heterogeneous microstructure, consisting of 2 components, the relatively regular and the amorphous random structures. Because the samples are completely transparent and the size of heterogeneous phase is very small, SR350 acted as a newtonian fluid (Fig. 2b). The molecular weight characterization of as-received SR350 helped us understanding the reason why low molecular weight component were evaporated as decomposition gas (see Section 3.2), and the good solubility in organic solvents, such as CH_2Cl_2 , in spite of a three-dimensionally cross-linked structure as received. The amorphous heterogeneous structure of SR350, determined from DSC, XRD, and rheological measurements, was also important for discussing the cause of deformation of SR350 phase at higher temperature (see Section of 3.3).

3.2. Decomposition gases and bulk composition as a function of pyrolysis temperature

The thermal decomposition was qualitatively characterized by the TGA-FTIR method, from room temperature to 1000°C. Fig. 3 compares the TGA curves of SR350 (as received), SR350 (after cross-linking by the amine catalysts), foamed PU, and foamed blend of SR350/PU. The reason, why SR350 (after cross-linking) is presented, is that the SR350 in foamed blend of SR350/PU is already cross-linked by the amine catalysts. Figs 4–6 display the FTIR results for the decomposition gases as a function of temperature for

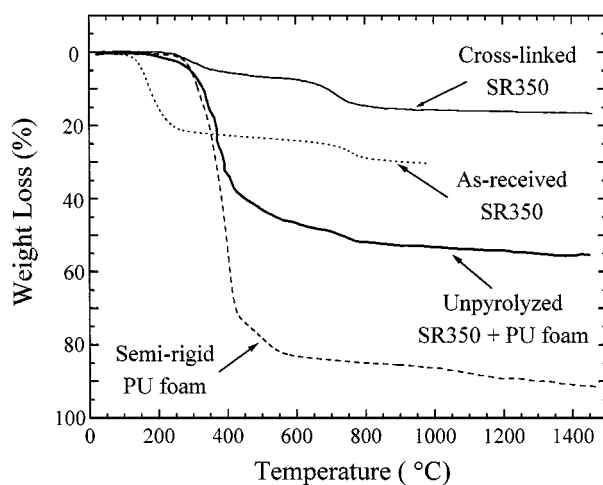


Figure 3 TGA curves of SR350 (as received), SR350 (cross-linked), foamed PU (unpyrolyzed), and foamed blend of SR350/PU (unpyrolyzed) under nitrogen.

SR350 (as received), foamed PU, and foamed blend of SR350/PU, respectively. The FTIR spectra were only reported for some typical temperatures to show more clearly the change of decomposition gases with increasing temperature, though FTIR measurements were performed every 25°C. It should be remembered that the IR technique can only detect the decomposition gases which are active for IR. H_2 or N_2 is inactive.

The thermal degradation of SR350 occurred in two steps, around 200 and 750°C (Fig. 3). The weight loss around 200°C was reduced by cross-linking. The FTIR

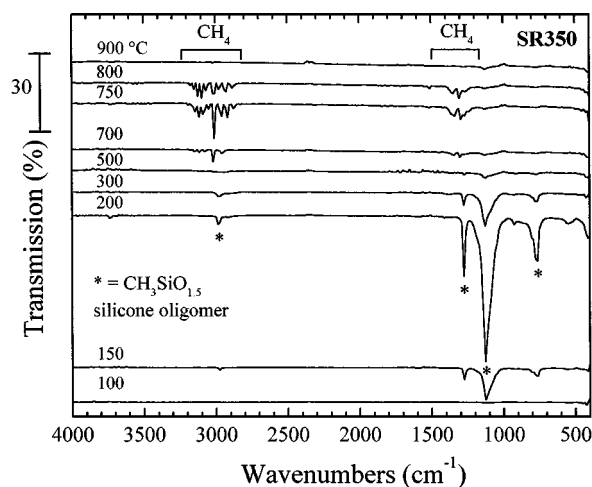


Figure 4 FTIR spectra of decomposition gases from SR350 (as received) with the TGA-IR method under nitrogen. Bands related to CH₄ and silicone oligomer are marked for clarity.

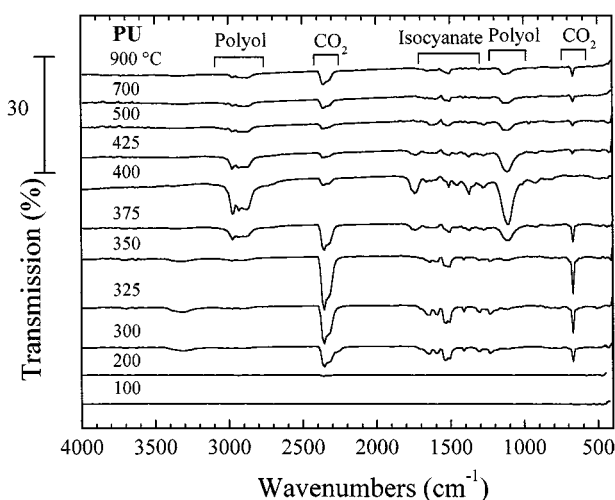


Figure 5 FTIR spectra of decomposition gases from foamed PU (unpyrolyzed) with TGA-IR method, under nitrogen. Bands related to CO₂, polyol and polyisocyanate are marked for clarity.

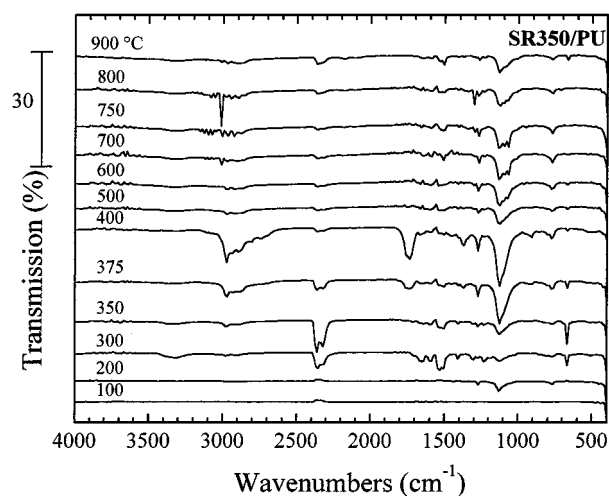


Figure 6 FTIR spectra of decomposition gases from the foamed blend SR350/PU (unpyrolyzed) with TGA-IR method, under nitrogen.

peaks at 200°C (Fig. 4), located at about 770, 1127, 1275 and 2980 cm⁻¹, can be attributed to Si-CH₃ (and Si-O) stretching, Si-O-Si asymmetric stretching, Si-CH₃ bending and C-H stretching, respectively. The

FTIR peaks at 750°C (Fig. 4), located at about 3016 and 1305 cm⁻¹, can be attributed to C-H stretching and C-H asymmetric stretching, respectively. Therefore, methyl silicone oligomers are part of the decomposition gas during the pyrolysis process around 200, and CH₄ was released around 750°C. The finding that in as-received SR350 oligomers are present is in good agreement with the GPC results, as well as with published literature for other silicone systems [26, 27]. The generation of water as by-product of the cross-linking reaction was not observed in the FTIR, probably due to its low amount.

The largest weight loss of foamed PU was observed between 300 and 500°C (Fig. 3). The FTIR of gas from decomposed foamed PU suggests two decomposition steps (Fig. 5). The first step is around 325°C, where the FTIR peaks located at about 668, 1511, and 2359 cm⁻¹ can be attributed to C=O asymmetric stretching, N-H bending (and C-N stretching), and C=O stretching (from CO₂), respectively. The second step is around 400°C, where the FTIR peaks, located at 1110, 1374, 1744 and 2974 cm⁻¹ can be attributed to C-O-C stretching, CH₂ wagging, C=O stretching (from carbonyl group), and CH₂ asymmetric stretching, respectively. The first decomposition step corresponds to the loss of low molecular weight components, mainly aliphatic fragments, resulting from the thermal degradation of the urethane linkages. During this step, the CO₂ trapped in closed cells (chemical blowing agent) is evolved. The by-products released in the second decomposition step derived mainly from the oligomeric isocyanate and high molecular weight polyether polyol. PU leaves 14 wt% of residue after TGA analysis under nitrogen, and this usually occurs when PU is three-dimensionally cross-linked [10–12]. The residue became almost zero after TGA up to 1000°C under air [10–12].

The decomposition behavior of a foamed blend of SR350/PU can be understood in its general aspect from the combination of that of SR350 and PU. The TGA curve of a foamed blend of SR350/PU, at temperatures higher than 400°C, is found to closely resemble the sum of that of its two components (Fig. 3). The foamed blend of SR350/PU did not display a large weight loss around 150°C, as is the case for as-received SR350. This can be explained considering that SR350 was pretreated at 150°C [11, 12], and cross-linked at room temperature because of the presence of amine catalysts in the starting solution [10]. Thus, the amount of low molecular weight SR350 would become much smaller, and this results in less gas evolution and weight loss around 200°C. In fact, the TGA curve for cross-linked SR350 shows virtually no weight loss up to 200°C. If one carefully observes the FTIR spectrum in Fig. 6, one can see peaks located at about 770, 1131 and 1275 cm⁻¹, at 375 and 400°C, which can be attributed to Si-CH₃ stretching, Si-O-Si asymmetric stretching, and Si-CH₃ bending, respectively. The peak at 1275 cm⁻¹ is close to the peak of decomposed gas of polyol at 1110 cm⁻¹, but the existence of peaks at 770 and 1175 cm⁻¹ proves that not only gas containing polyols but also gas containing methylsilicone are generated around 375°C. We can thus infer that the temperature at which the gas of methylsilicone is generated increases from 200 to 375°C, because of the

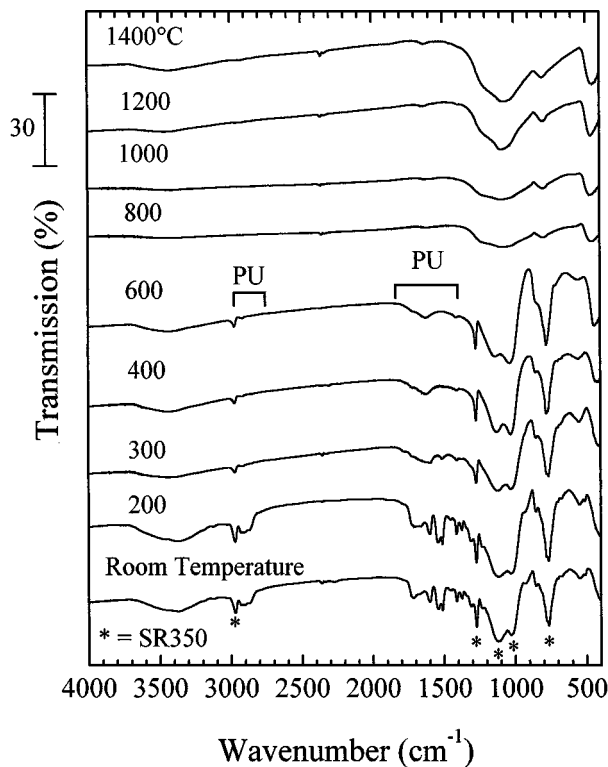


Figure 7 FTIR spectra of SR350/PU foam after pyrolysis at various temperatures. Bands related to polyurethane and silicone resin are marked for clarity.

cross-linking reaction of SR350 in the presence of amine catalyst. Fig. 7 represents the thermal evolution of a foamed blend of SR350/PU at different pyrolysis temperatures. All the FTIR peaks at room temperature can be attributed to the blend structure of SR350/PU. Note the absence of peaks attributable to the Si-OH bond (at about 900 cm^{-1}), indicates the cross-linking of the silicone resin in the blend [10]. From Fig. 7, obvious step-changes of the FTIR spectrum are observed at 300 and 800°C . Below 300°C the chemical composition of the material consists merely of the blend of SR350/PU, while above 300°C only SR350 was left (reflections attributable to bonds in the PU component gradually disappear in the 400 to 600°C range, because of pyrolytical decomposition). At temperatures higher than 800°C , the two sharp peaks, located at 1269 cm^{-1} (Si-CH₃ bending) and at 761 cm^{-1} (Si-CH₃ stretching), are disappeared because of the polymer-to-ceramic transformation in the silicone resin occurring with the generation of CH₄ and hydrogen gas, and only two major peaks, located at about 800 cm^{-1} (Si-C stretching) and at about 1080 cm^{-1} (Si-O stretching), are left. The step-change features concerning the composition of the material and the fact that there are two key temperatures in the thermal process are in agreement with the FTIR gas analysis during the pyrolysis of foamed blend of SR350/PU as well as with the curves for the weight loss versus pyrolysis temperature. The FTIR spectra in the $1000\text{--}1400^\circ\text{C}$ range are similar to what is reported in the literature for a silicon oxycarbide glass [7, 26].

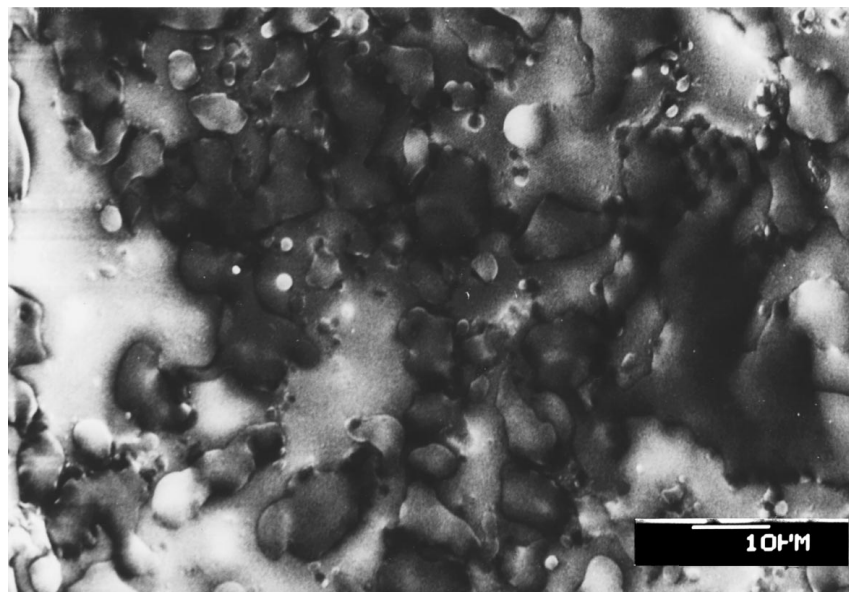
From the point of view of decomposition gases and of the composition of the material, the thermal evolution from foamed blend of SR350/PU to ceramic foam can be reasonably explained by considering two main

effects, the polymer-to-ceramic conversion of SR350 (at temperatures higher than 600°C) and the decomposition of PU (at temperatures lower than 400°C). From the TGA curves (Fig. 3) it can be seen that the data related to the unpyrolyzed foamed blend (about 54% weight loss at 1200°C) are in good agreement with the computed sum of the losses coming from the PU (about 89.2% weight loss at 1200°C) and silicone resin (about 16.1% weight loss at 1200°C , after crosslinking) components. Chemical analysis confirmed the presence of excess free carbon in the pyrolyzed foams, coming from the incomplete decomposition of PU, compared to SiOC ceramic produced from pure SR350 [11, 12].

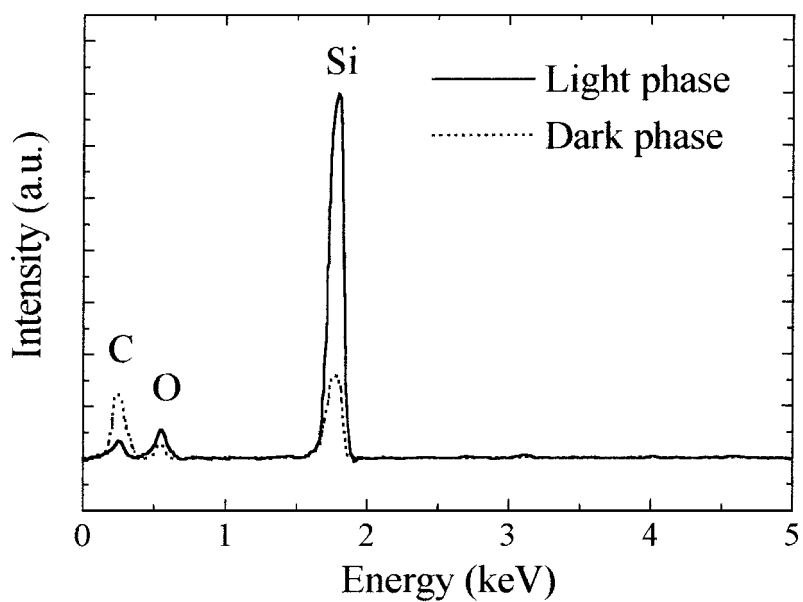
3.3. Evolution of the phase-morphology with pyrolysis temperature

The compositional morphology of cell wall surface in foamed blends of SR350/PU before pyrolysis was investigated with SEM. It has already been reported that foams obtained with this process possess about 30% of open-cell in the as prepared stage [10–12], through which decomposition gases can flow. Fig. 8a shows the photo of a cell wall surface in a foamed blend of SR350/PU before pyrolysis, by using backscattered electrons. In Fig. 8a islands, with a dimension of about $5\text{--}10\ \mu\text{m}$, were dispersed in a matrix phase. At this stage, one can not say whether PU is domain or matrix. Fig. 8a suggests that the blend of SR350/PU is not miscible but has the sea/island morphology that is typical of a phase-separated structure. The phase morphology of polymer blends has been extensively studied, and it is known that only for limited combinations a complete miscibility, i.e. a one phase structure can be achieved [39]. From the miscibility point of view [39], therefore, it would be quite natural for polyurethane and methyl-silicone resins to have a two-phase structure, mainly because of the difference of their surface tension (methyl-silicone resin 23 dyne/cm, polyurethane 38 dyne/cm) [9, 40].

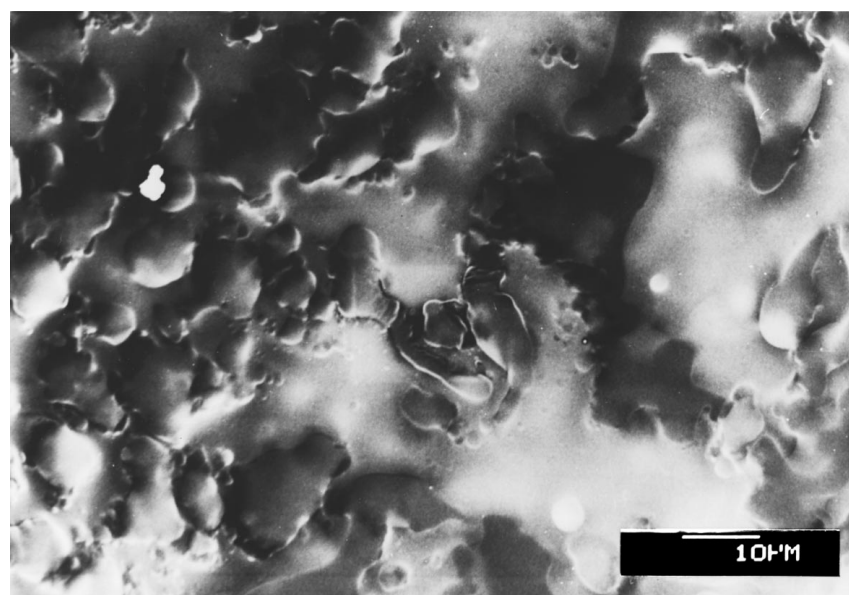
The elemental analysis was performed for both the island domain and the matrix area to identify which phase is PU in Fig. 8a. As shown in Fig. 8b, the light matrix area contains Si, C and O, while in the dark island domain area the Si signal is much less evident and the C signal is the main one. We can thus safely state that the matrix is comprised of SR350, while the particle domain is PU. The reason why the elemental analysis shows a small amount of Si for the dark domain areas could be that SR350 covers the outer surface wall, or that the electrons that gave rise to the signal traveled through the depth of the PU islands (being mostly comprised of the light element C) and hit some part of the SR350 matrix underneath. This result was quite unexpected, since PU was intended to be used as a sacrificial template matrix for generating a foam structure. From the phase-morphology investigations of blends of two polymers having the same volume, it is known that the polymer with the lower viscosity becomes the matrix [39]. For realizing a good foamed structure, i.e., with uniform cell size and large expansion by foaming, studies about foam processability, rheology and polymer structure suggest that polymers with sufficient



(a)

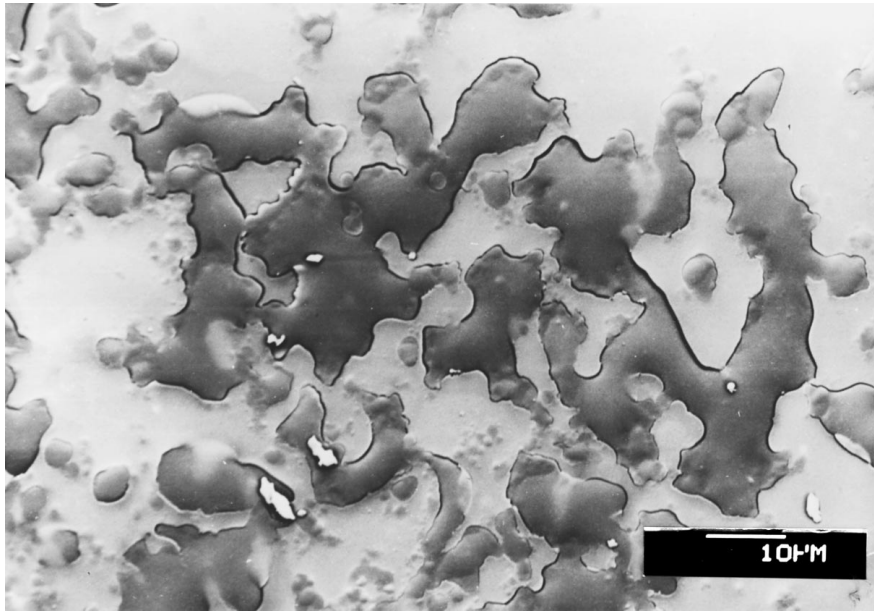


(b)

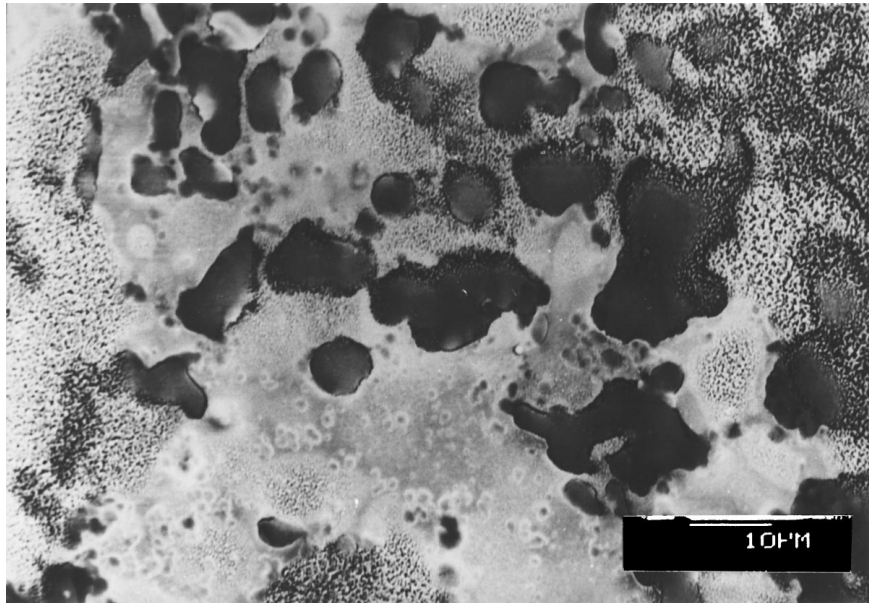


(c)

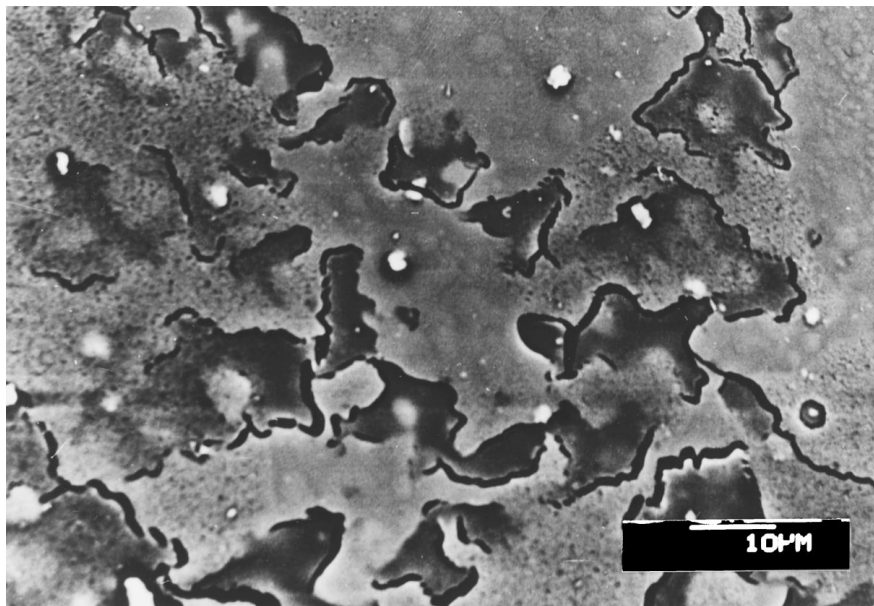
Figure 8 SEM micrographs of the cell surface of SR350/PU foam; backscattered electrons. Samples pyrolyzed at different temperatures: (a) unpyrolyzed, (b) EDX analysis of SR350/PU foam (unpyrolyzed), (c) 200°C, (d) 300°C, (e) 400°C, (f) 600°C, (g) 800°C, (h) 1000°C, (i) 1200°C, (j) 1400°C. (Continued)



(d)

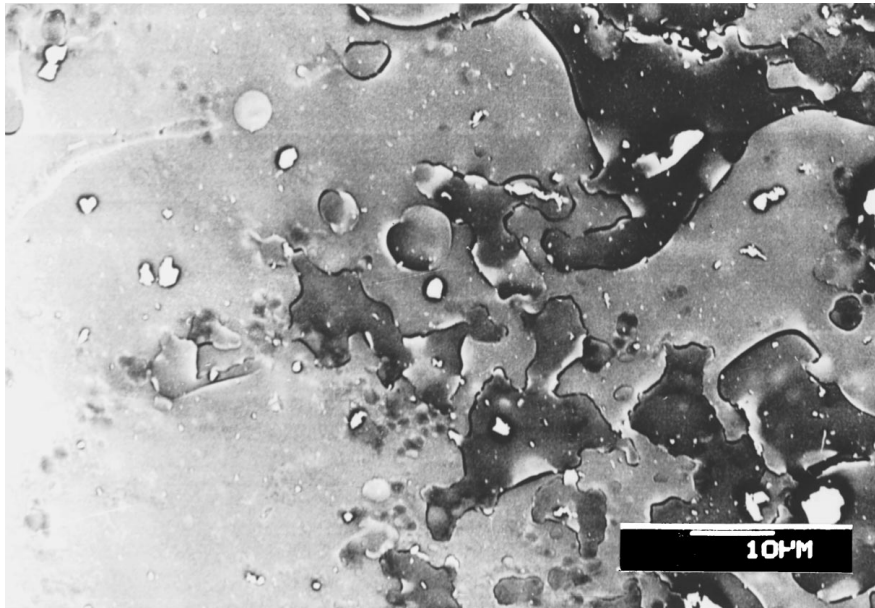


(e)

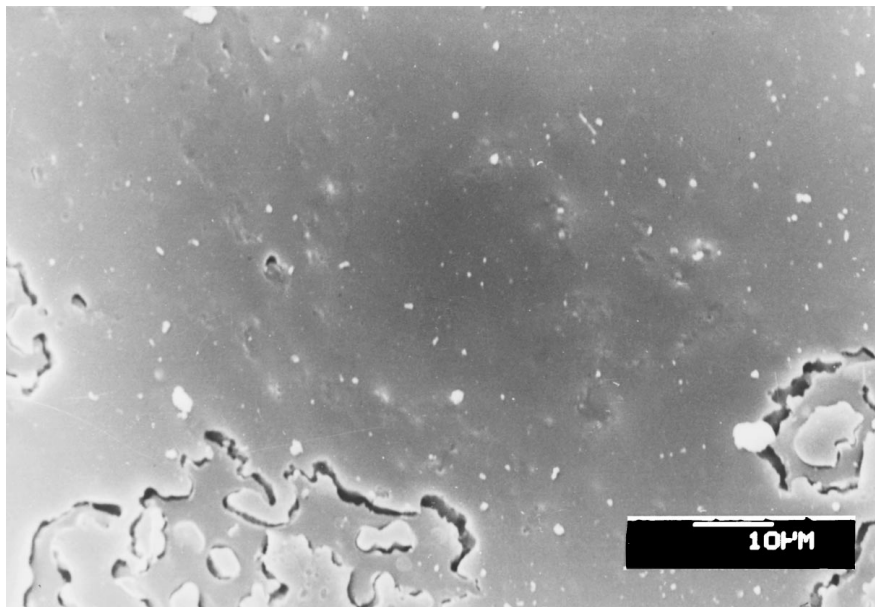


(f)

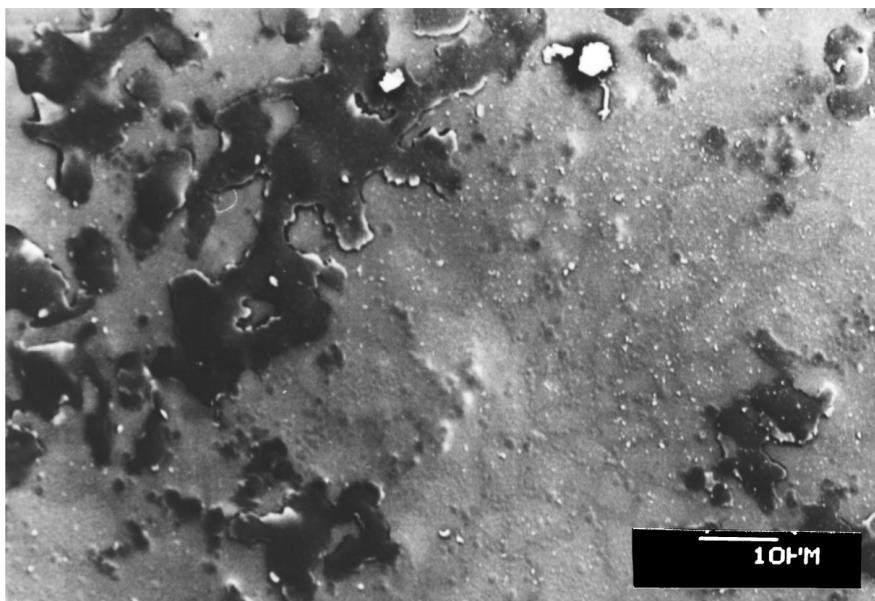
Figure 8 (Continued).



(g)

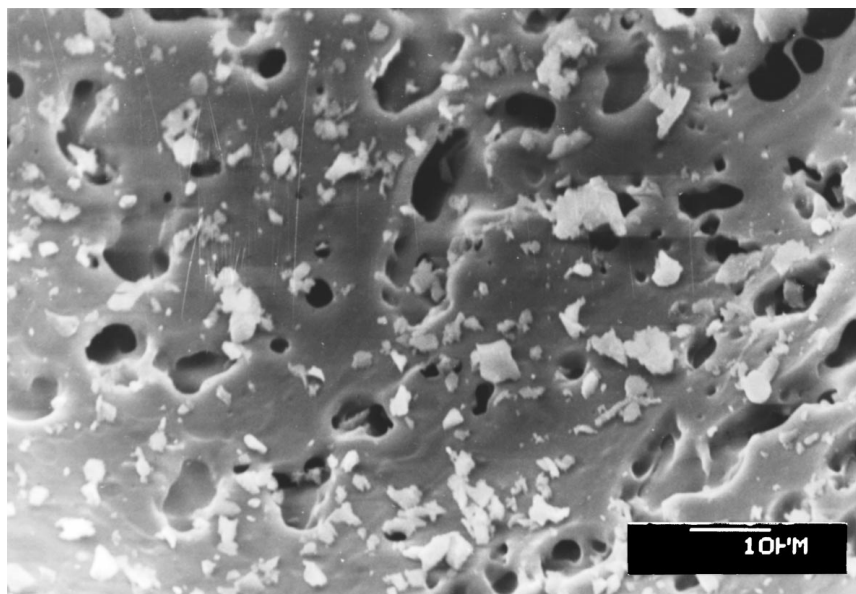


(h)



(i)

Figure 8 (Continued).



(j)

Figure 8 (Continued).

viscosity to sustain cell structure under elongational deformation are required [31, 41]. It is evident that the cross-linking reaction occurring in the low viscous silicone resin solution helps to achieve higher viscosity, and that PU rigidizes by polyol and isocyanate reaction. By taking these facts into consideration, it seems thus that the cross-linked SR350 satisfies the above requirements, so that SR350 can become the matrix and stable foams with good morphology can be produced.

Fig. 8 from c to j show the evolution with pyrolysis temperature of the morphology of the two-phase structure in the wall surface of foams. According to the SEM investigation, the morphology changes that occur during pyrolysis can be divided into three steps. In the first step, from room temperature up to 300°C, the PU particle domains become closer and aggregated to each other. In the second step, for pyrolysis temperatures up to 1200°C, the PU domain areas become smaller and tend to disappear. Elemental analysis confirmed the attribution of the dark particles to PU at all pyrolysis temperatures. Published literature concerning the production of porous silicate from the pyrolysis of organic/inorganic polymer blends confirm that the interconnected organic polymer disappears and the inorganic polymer skeleton structure is always left [20–23]. It was rather unexpected to observe that, during pyrolysis, the cell wall surface was always mostly smooth without holes from the disappearance of PU, considering that SR350 polymer was rigidized by the above mentioned cross-linking reaction. It seems, in fact, that the SR350 matrix is able to deform during the disappearance of PU. In the third region, heating above 1200°C, many small holes (about 5 μm) were generated. This can be attributed to the carbothermal reduction reactions occurring in the SiOC ceramic [26].

It is useful, at this point, to discuss the two-phase morphology evolution occurring in each step. The observations for the first region suggest that the difference of surface tensions of the SR350 and PU enhances the aggregation of PU to minimize the interfacial area.

It seems evident that both PU and SR350 phases deformed during heating, since their surface was always smooth. From this fact, we infer that SR350 has a cross-linked structure, but can still be deformed. One probable reason is that the heterogeneous microstructure of SR350, or the structure (RSiO_{1.5}) deriving from three-functional silicate monomers, hinders a complete rigid cross-linking.

The decrease of the PU phase in the second region is expected because of its decomposition (see TGA analysis). However, it is very important to note that the wall and the struts of the foams are not broken by the release of degradation gases from the PU. They remain mostly smooth and dense, without any formation of pores. This can be explained considering that the PU domains become interconnected, creating a porous structure through which the degradation gases can escape, and that the wall and strut thickness is relatively small, around 20–50 μm, thus allowing gas permeation. Moreover, the polymer-to-ceramic conversion of SR350 is occurring during the disappearance of PU, and it is known that some open porosity develops in the early stages of this process [3, 13].

It is interesting in this context to discuss the difference between two systems using organic polymer/ceramic blends [20, 22, 23] as starting materials under comparable pyrolysis conditions (400–1000°C). The elimination of the organic part in organic/inorganic hybrid leaves pores whose sizes are similar to that of original organic phase [20, 22, 23], while in the SR350/PU case it leads to a dense structure. In the former case, the ceramic component is SiO₂ deriving from four functional silicate monomers (alkoxides). On the other hand, the present ceramic (inorganic) part (SR350) consists of mostly three functional silicate monomers, and has the heterogeneous structures which were discussed earlier (see XRD and rheological studies). The less functional monomer structures of SR350 than that of SiO₂ could be regarded as the cause for the deformation of SR350 during pyrolysis of PU, a process that

does not leave residual porosity. It would be significant to control the rigidity of ceramic parts for designing unique ceramic structures, like macroporous materials (e.g. a foam) with a microporous microstructure (i.e. microporous cell walls), that could be useful for sensors/catalysis applications. Further experiments will be required to explore and exploit this possibility in detail.

The results concerning phase-morphology raise questions regarding the role of PU in the process. From previous experiments one knows that PU (actually mainly the polyol component) is essential for giving the shape to the cells: in fact the use of flexible, semirigid or rigid PU affords different morphologies to the ceramic foam

[11, 12]. It was thus expected it to form a continuous interpenetrating phase within the SR350/PU blend, a hypothesis that the current data do not support, since PU displays rather a sea-island morphology. It can be proposed from our findings that PU is active in controlling the morphology of the foam in the early stages of the foaming process, when there is still sufficient solvent to allow a mixing of viscous PU and SR350. Phase separation with a sea-island morphology then would occur when the foam solidifies. To confirm the role of the polyurethane in the process and to simplify the technology for possible industrial applications, a drastic reduction of the PU/SR350 ratio would be worthwhile investigating. These further experiments will be carried out and reported elsewhere.

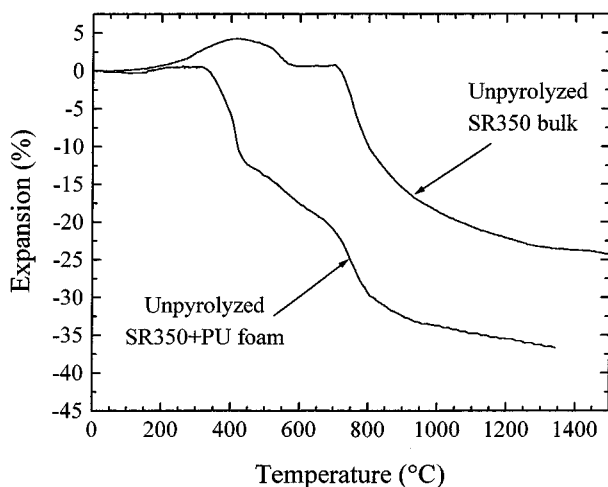


Figure 9 Expansion as a function of pyrolysis temperature for unpyrolyzed SR350 bulk and unpyrolyzed SR350/PU foam.

3.4. Change of dimension and apparent bulk density with pyrolysis temperature

It is interesting how dimension and bulk density change with pyrolysis temperature. Fig. 9 shows the linear expansion with pyrolysis temperature of an as-prepared SR350/PU foam and an as-received SR350 resin. The dimensional change can be easily interpreted considering that the decomposition of the PU and the polymer-to-ceramic conversion for the SR350 resin. The two processes are mainly active in the 300 to 400°C range and in the 650 to 800°C range, respectively (see Figs 3 and 7). Furthermore, the polymer-to-ceramic transformation, that occurs with CH_4 and H_2 gas generation, bond redistribution (exchanging of Si-O and Si-C bonds), and carbo-thermal reduction

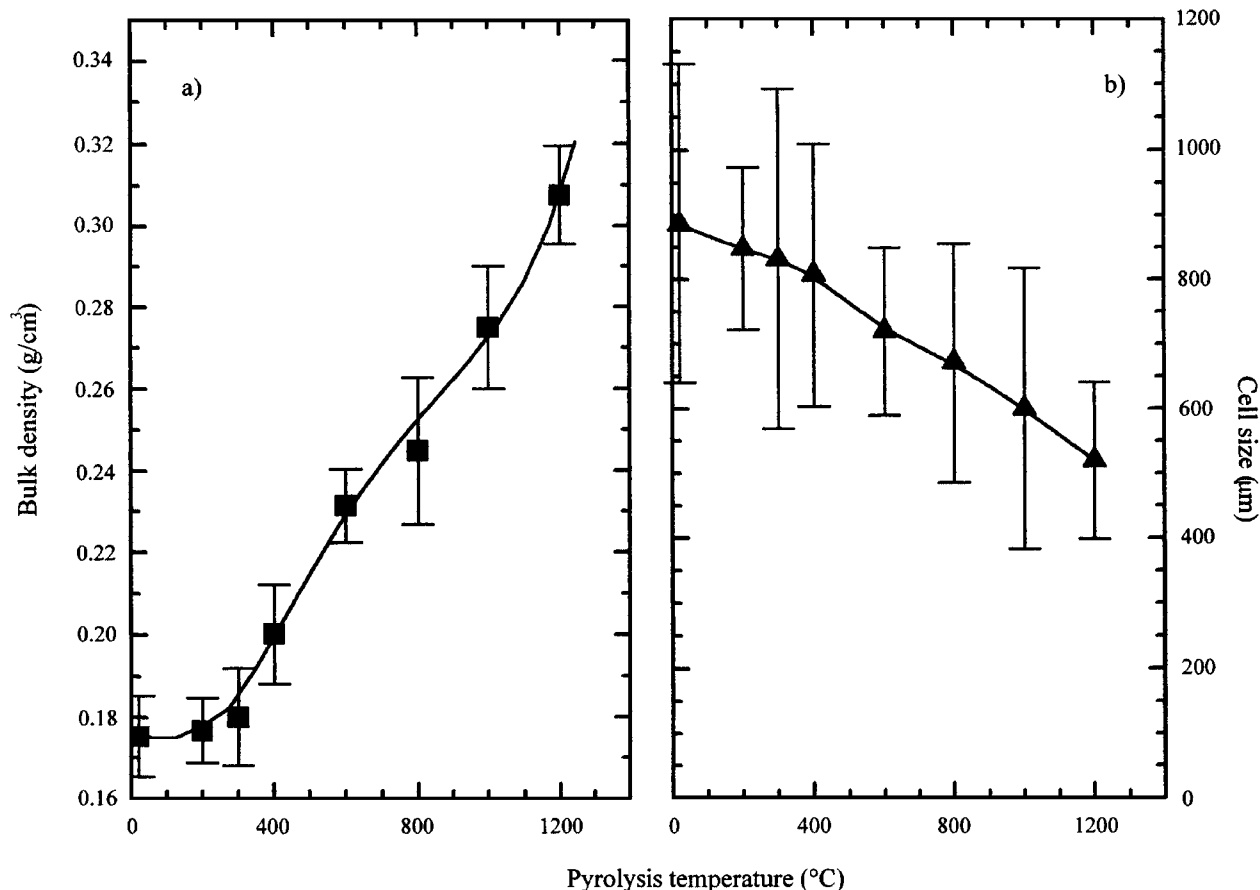


Figure 10 (a) Bulk density and (b) cell size as a function of pyrolysis temperature for unpyrolyzed SR350/PU foam.

reactions (at $T > 1300^{\circ}\text{C}$), involves a densification of the material (true density varies from about 1.1 to about 2.12 g/cm^3) [2–4, 26]. The two step-changes were seen in the shrinkage of SR350/PU foam around 300 and 800°C (Fig. 9). The shrinkage characteristics observed were, in fact, in good agreement with the TGA curves (see Fig. 3) and with the FTIR results (see Fig. 7).

Fig. 10 displays the apparent bulk density and the cell size of foamed blend of SR350/PU as a function of pyrolysis temperature. The bulk density changed from 0.17 to 0.31 g/cm^3 during pyrolysis from room temperature to 1200°C . The increase of bulk density clearly started around 400°C (temperature at which most of the PU has disappeared), while average cell size varied with pyrolysis temperature without major step-changes. The cell size shrank about 35% up to 1200°C , which is in good agreement with the shrinkage measured by dilatometry (Fig. 10). It is noteworthy to point out that the shrinkage occurred in all the directions with the same degree (isotropic shrinkage) [11, 12].

4. Conclusions

The novel process from a foamed blend of silicone resin/polyurethane to ceramic foam utilizes an organic polymer as processing aid that disappears during pyrolysis. The TGA-FTIR, SEM, and dilatometry results were all consistent with respect to the interpretation of the evolution of the material with pyrolysis temperature due to the concurrent decomposition of the PU component and the polymer-to-ceramic transformation of the silicone resin. SEM analysis demonstrates that the foamed blend before pyrolysis had a sea/island type phase-separated morphology, where the silicone resin constituted the matrix. It was quite unexpected that the PU phase was dispersed as particles in the SR350 matrix, and it was observed that it became aggregated and finally disappeared with increasing temperature. At high temperatures, a macroporous SiOC ceramic material with dense cell walls and struts was left. The densification mechanism must involve the deformation of the cross-linked silicone resin matrix during pyrolysis. The role of PU in the process can be regarded as an essential processing aid for controlling the structure of the foams at room temperature, while the silicone resin can act as an effective matrix to provide a dense foamed ceramic structure.

Acknowledgments

T.T. and H.M. acknowledge the financial support of Deutsche Forschung Gemeinschaft (DFG). P.C. and M.M. acknowledge the support given by the Vigoni program.

References

1. R. W. RICE, *Am. Ceram. Soc. Bull.* **62** (1983) 889.
2. R. BANEY and G. CHANDRA, "Encyclopedia of Polymer Science and Engineering, Preceramic polymers" (John Wiley & Sons, New York, 1988) p. 312.
3. R. RIEDEL, "Materials Science and Technology, Advanced Ceramic from Inorganic Polymers" (VCH, Weinheim, 1995) p. 1.
4. J. BILL, F. WAKAI and F. ALDINGER, "Precursor-Derived Ceramics" (WILEY-VCH, Weinheim, 1999) p. 59.
5. S. YAJIMA, J. HAYASHI, M. OMORI and K. OKAMURA, *Nature* **261** (1976) 683.

6. D. A. WHITE, S. M. OLEFF, R. D. BOYER, P. A. BUDINGER and J. R. FOX, *Adv. Ceram. Mat.* **2** (1987) 45.
7. D. A. WHITE, S. M. OLEFF and J. R. FOX, *ibid.* **2** (1987) 53.
8. R. H. BANEY, M. ITOH, A. SAKAKIBARA and T. SUZUKI, *Chem. Rev.* **95** (1995) 1409.
9. M. TANIMURA, "Handbook of Silicone Materials" (Toray Dow Corning Silicone, Tokyo, 1993) p. 281.
10. P. COLOMBO, M. GRIFFONI and M. MODESTI, *J. Sol-gel Sci. Tech.* **13** (1998) 195.
11. P. COLOMBO and M. MODESTI, *J. Amer. Ceram. Soc.* **82** (1999) 573.
12. *Idem.*, *J. Sol-gel Sci. Tech.* **14** (1999) 103.
13. P. GREIL, *J. Amer. Ceram. Soc.* **78**(4) (1995) 835.
14. S. WALTER, D. SUTTOR, T. ERNY, B. HAHN and P. GREIL, *J. Eur. Ceram. Soc.* (1996) 387.
15. T. GAMBARYAN-ROISMAN, M. SCHEFFLER, T. TAKAHASHI, P. BUHLER and P. GREIL, *EUROMAT 99* Munich, in press.
16. K. SAITO, Y. ARAKIDA and M. INOUE, "Injection Molding Technology of Fine Ceramics" (Nittkan Kogyou Shinbun, Tokyo, 1987) p. 213.
17. G. S. GRADER and L. ZURI, *J. Amer. Ceram. Soc.* **76** (1993) 1809.
18. P. SEPULVEDA, *Amer. Ceram. Soc. Bull.* **76** (1997) 61.
19. J. SAGGIO-WOYANSKY, C. E. SCOTT and W. P. MINNEAR, *ibid.* **71** (1992) 1674.
20. S. SATO, T. MURAKATA, T. SUZUKI and T. OHGAWARA, *J. Mater. Sci.* **25** (1990) 4880.
21. K. NAKANISHI and N. SOGA, *J. Amer. Ceram. Soc.* **74** (1991) 2518.
22. Y. MORIYA, M. SONOYAMA, F. NISHIKAWA and R. HINO, *J. Ceram. Soc. Jpn.* **101** (1993) 518.
23. M. MOTOMATSU, T. TAKAHASHI, H. Y. NIE, W. MIZUTANI and H. TOKUMOTO, *Polymer* **38** (1997) 177.
24. R. K. ILLER, "The Chemistry of Silica" (John Wiley & Sons, New York, 1979) p. 172.
25. L. C. KLEIN, "Sol-gel Technology for Thin Films, Fibers, Preforms, Electronics, and Specialty Shapes" (Noyes Publishers, New Jersey, 1988) p. 2.
26. G. R. RENLUND, S. PROCHAZKA and R. H. DOREMUS, *J. Mat. Res.* **6** (1991) 2716.
27. V. BELOT, R. J. P. CORRIU, D. LECLERCQ, P. H. MUTIN and A. VIOUX, *J. Polym. Sci. Part A Polym. Chem.* **30** (1992) 613.
28. F. I. HUWITZ, P. HEIMANN, S. C. FARMER and D. M. HEMBREE JR., *J. Mater. Sci.* **28** (1993) 6622.
29. M. J. WILD and P. BUHLER, *ibid.* **33** (1998) 5441.
30. J. D. FERRY, "Viscoelastic Properties of Polymers" (John Wiley & Sons, New York, 1980) p. 264.
31. C. W. MACOSKO, "Rheology; Principles, Measurements, and Applications" (VCH Publishers, New York, 1994) p. 285.
32. T. TAKAHASHI, J. KASCHTA and H. MÜNSTEDT, *Rheol. Acta*, submitted.
33. S. SAKKA, "Fundamentals and Applications of Glass Science" (Uchida Roukakuho Publishing Co., Ltd., Tokyo, 1997) p. 5.
34. J. F. BROWN JR., L. H. VOGT JR., A. KATCHMAN, J. W. EUSTANCE, K. M. KISER and K. W. KRANTZ, *J. Am. Chem. Soc.* **82** (1960) 6194.
35. S. WU, *J. Polym. Sci. Part B Polym. Phys.* **27** (1989) 723.
36. S. ONOGI, T. MASUDA and K. KITAGAWA, *Macromolecules* **3** (1970) 109.
37. F. CHAMBON and H. H. WINTER, *J. Rheol.* **31** (1987) 683.
38. T. SHIKATA and D. S. PEARSON, *ibid.* **30** (1994) 601.
39. L. A. UTRACKI, "Polymer Alloys and Blends, Thermodynamics and Rheology" (Carl Hanser Verlag, Munich, 1989) p. 131.
40. J. BRANDRUP, E. H. IMMERGUT, "Polymer Handbook," 3rd ed. (John Wiley & Sons, New York, 1989) p. VI/422.
41. H. MÜNSTEDT, S. KURZBECK and L. EGERSDÖRFER, *Rheol. Acta* **37** (1998) 21.

Received 26 April
and accepted 26 September 2000